Core excitons in Na *K* photoabsorption of NaF: Resonant Auger spectroscopy

A. Kikas, E. Nõmmiste, R. Ruus, and A. Saar
Institute of Physics, University of Tartu, Riia 142, 51014 Tartu, Estonia

I. Martinson
Department of Atomic Spectroscopy, Lund University, Professorsgatan 1, S-22100 Lund, Sweden
(Received 19 May 2001; published 28 November 2001)

The nature of Na 1*s* photoabsorption in NaF is investigated by using the resonant Auger decay of Na 1*s* core excitations. The appearance of peaks in the Auger spectra, when the energy of excitation coincides with the photoabsorption thresholds, shows that, despite the absence of pronounced structures in photoabsorption spectra, core excitons are created in the threshold region of the Na 1*s* x-ray-absorption spectrum. The core exciton excited at a photon energy of 1076.8 eV originates from $1s^{-1}3p$ states similarly to the atoms of Ne and Na. The role of the dipole-forbidden transitions to the $1s^{-1}3s$ and $1s^{-1}3d$ states in the formation of the double structure at 1073.7 and 1074.7 eV is discussed.

DOI: 10.1103/PhysRevB.64.235120 PACS number(s): 78.70.Dm, 32.80.Hd

I. INTRODUCTION

High-resolution inner-shell photoabsorption spectra provide a rich source of information about the electronic structure and chemical bonding of compounds. If an x-ray photon is absorbed in a solid, a core electron is excited to an empty conduction state, or to an empty state below the ionization threshold. In the latter case an electron–core-hole bound state, a core exciton, is formed which manifests itself as pronounced structures in the pre-edge region of the x-ray-absorption (XAS) spectrum. However, in many cases the electron–core-hole interaction is so strong that in a wide energy region the XAS is almost entirely excitonic in nature. In particular, this is the case of XAS of alkali cations in alkali halides, where the electron–core-hole interaction is overwhelmingly large since the core hole in the alkali ion is not effectively screened by the valence-electron cloud which lies almost completely on the halogen ions.[1] Recently electron–core-hole interactions were explicitly included into theoretical calculations of XAS by Shirley[2] and Buczko *et al.*[3] They have shown that the inclusion of the electron-hole interaction dramatically affects the XAS results, and essentially improves the agreement with the experiment for insulators and semiconductors.

The development of synchrotron radiation technology has provided a powerful tool to study the properties of core excitations through their decay products.[4–6] The decays of these autoionizing states are dominated by resonant Auger transitions which involve inner-shell electrons, with the resonantly excited electron remaining in its orbital as a ''spectator.'' Since a localized excited electron screens the final-state core holes, the kinetic energy of the resulting Auger electrons is higher than in the case of the decay of an ionized state.

Due to its simple, neonlike electronic structure ($1s^2 2s^2 2p^6$), sodium 1*s* photoabsorption in sodium halides is a widely investigated test system. In the spectra of most sodium halides there is the sharp peak below the photoionization threshold, showing the existence of core excitons in the pre-edge region. An exception to this is NaF, where the first main absorption feature of the Na 1*s* XAS is a rather broad maximum, the origin of which appears to be ambiguous.

The aim of this paper is to study experimentally the role of electron–core-hole bound states in the Na 1*s* XAS of NaF. We present a set of resonant Na *KLL* Auger spectra in the vicinity of the Na 1*s* edge in NaF. These spectra exhibit spectator resonant Auger structures at photon energies of 1073.7, 1074.7, and 1076.8 eV. This shows that the core excitons are created at these photon energies, despite the absence of pronounced structures in the threshold region of the Na 1*s* XAS.

II. EXPERIMENT

The experiments were carried out at the beamline D1011 at the MAX-II storage ring in MAX-Lab (Lund University, Sweden). The beamline is equipped with a Zeiss SX 700 plane grating monochromator and a Scienta SES-200 hemispherical electron energy analyzer. The monochromator resolution was about 0.6 eV (corresponding to 6-μm slits at the Na *K* edge) and the electron energy resolution was 0.3 or 0.15 eV (using 300- and 150-eV pass energies, respectively). The sample specimens of a thin film (about 10-nm thickness) were deposited on a stainless-steel substrate by a vacuum evaporation technique. This thickness would be enough to effectively avoid the influence of charging on the electron spectra. Pressures during evaporation did not exceed 10^{-7} mbar. Samples with fresh surfaces were transported *in situ* to an experimental chamber with a base pressure of 10^{-10} mbar.

The electron spectra are presented on an energy scale where the zero binding energy corresponds to the bottom of the conduction band. The energy scale was established by measuring the photoemission binding energies with respect to the top of the valence band, and by subsequently adding the optical band-gap energy of NaF [11.6 eV (Ref. 7)]. The binding energies of the photoelectron lines, obtained in this work, are listed in Table I.

 ©2001 The American Physical Society

TABLE I. Binding energies of the energy levels of NaF relative to the bottom of the conduction band.

Level	Binding energy, eV
Top of VB	11.6
VB (F 2*p*)	13.1
F 2*s*	33.6
Na 2*p*	35.8
Na 2*s*	68.5
F 1*s*	689.6
Na 1*s*	1076.7

III. RESULTS AND DISCUSSION

A. Photoabsorption

The Na 1*s* XAS is presented in Fig. 1. The spectrum was obtained by measuring the total photocurrent through the sample. The main features of the photocurrent spectrum in Fig. 1 are in accordance with the earlier experimental investigations of the Na 1*s* photoabsorption via the optical density spectrum,[8] the electron yield spectrum,[9] and the partial electron yield spectrum of the Auger electrons[10] of NaF. Note that in previous x-ray-absorption experiments a shoulder structure was observed for the Na 1*s* threshold, but the double-band structure was unresolved.[9] For the calculation of the Na 1*s* photoabsorption, mainly a multiple-scattering approach was used,[8–10] but the best agreement between the experimental and the calculated XAS of NaF was achieved by Shirley *et al.*,[11] who used a band-structure-based approach, including electron–core-hole interactions. This confirms that despite the absence of sharp peaks in the threshold region of the absorption spectrum, the excitonic effects play an important role in the Na 1*s* photoabsorption of NaF.

At first glance, it seems that the main features in the photoabsorption spectrum are located above the ionization limit of the 1*s* level, 1076.7 eV. This estimate is obtained by adding the band-gap energy to the energy difference between the Na 1*s* core level and the top of the valence band (also see Sec. II and Table I). This procedure was originally suggested by Pantelides.[1] However, it uses data obtained from optical measurements. It is clear that the effect of the Na 1*s* core hole on the conduction band is different from that on the hole in the valence band and, consequently, the use of the optical-band-gap value decreases the reliability of the results obtained by this procedure. Thus the exact position of the ionization limit of the 1*s* level remains uncertain, and the existence of bound states above 1076.7 eV cannot be *a priori* excluded. Therefore, the photon energy region around this threshold energy is the most probable area where electron-core–hole bound states may be observed in a resonant Auger experiment.

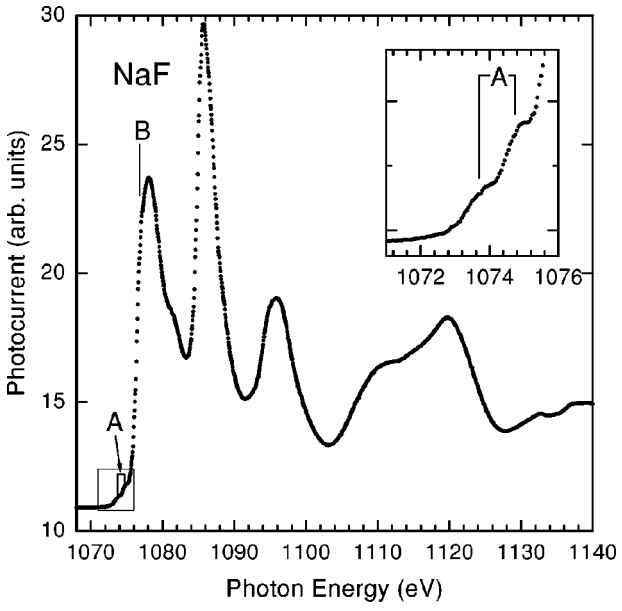

FIG. 1. Na *K* photoabsorption in NaF.

B. Resonant Auger spectra

For an overview, Fig. 2(a) shows the energy distribution curves (EDC's) recorded at different photon energies around the Na 1*s* absorption edge (shown in the inset). The origin of different peaks is indicated. The uppermost curve in Fig. 2(a) shows the so-called ''normal Auger'' spectrum, excited by 1200-eV photons, i.e., the excitation energy is far above the core-level threshold. The normal Auger spectrum exhibits three well-separated groups of peaks, which is typical of *KLL* Auger spectra. In more detail, there is a $KL_1L_1(^1S)$ band at 917 eV, $KL_1L_{23}(^1P)$ and $KL_1L_{23}(^3P)$ bands at about 946 and 958 eV, respectively, and a $KL_{23}L_{23}(^1D)$ main line at 985 eV together with a $KL_{23}L_{23}(^1S)$ shoulder at its low-kinetic-energy side. The spectra displayed in Fig. 2(a) were measured with the electron energy resolution of 150 meV. This set of curves shows, comparatively well, the principal $KL_{23}L_{23}(^1D)$ peak; however, there is no sufficient statistics concerning weaker details in the prethreshold spectra. Therefore, to show the weak prethreshold spectra in detail, in Fig. 2(b) we present the EDC's of NaF obtained by setting the energy resolution of the electron spectrometer to 300 meV. The electron spectra in Fig. 2(b) are displayed on a binding-energy scale, and the Na 2*s* photoelectron line is well seen due to its constant binding energy. On the kinetic-energy scale [Fig. 2(a)], this photoelectron line shifts to higher kinetic energies in proportion to the increasing photon energy, its intensity remaining constant within experimental uncertainties.

Figure 3 shows the photon energy dependence of the integrated intensities of the selected Auger peaks. These intensities have been obtained by a curve-fitting from the spectra presented in Figs. 3(a) and 3(b). Note that the photon energy dependence of the intensity of the main $KL_{23}L_{23}$ Auger peak [Fig. 3(c)] is similar to the photoabsorption spectrum [Fig. 3(d)].

One can see in Figs. 2(a) and 2(b), that, with increase of the photon energy, in the electron spectrum there appears a new peak [denoted by *a* in Fig. 2(a)]. Its energy position is slightly higher than the energy of the main $KL_{23}L_{23}(^1D)$ Auger peak. This satellite shifts to higher kinetic energies with the increase of the photon energy [see Fig 2(a)], while

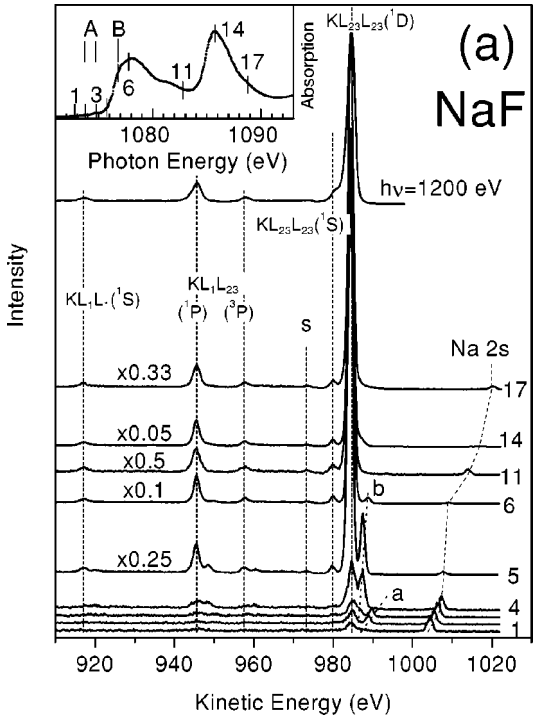

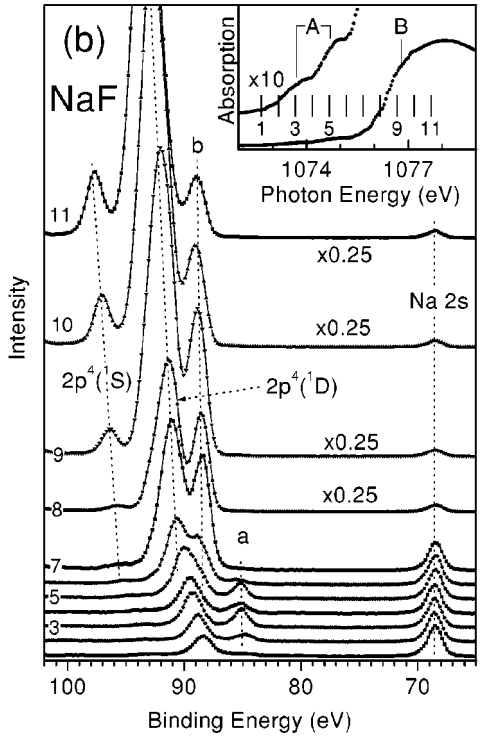

FIG. 2. Resonant Auger spectra of NaF at the Na 1*s* photoabsorption edge. Panel (a) gives an overview of the spectra, measured by using a 150-eV pass energy. Panel (b) shows the spectra in the prethreshold region, measured by using a 300-eV pass energy. In the insets the photoabsorption spectrum is shown, the numbers marking the photon energies used to measure the resonant Auger spectra. The final states of the corresponding spectral structures are labeled in the figure.

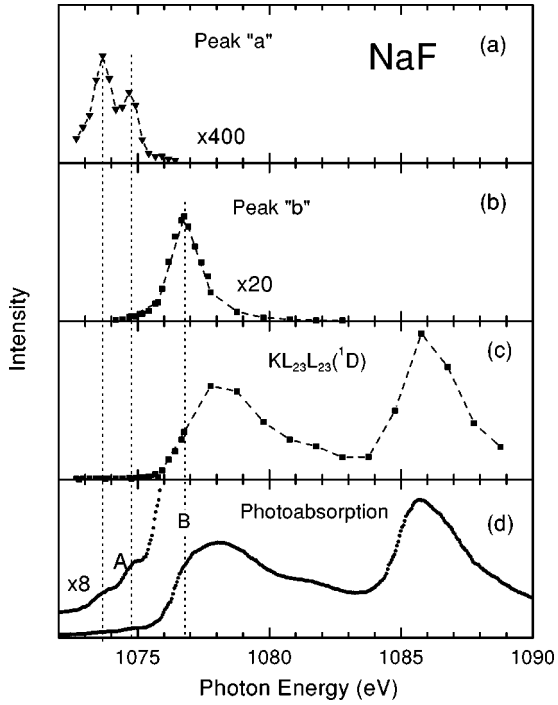

FIG. 3. The excitation energy dependence of peak intensities in the Na 1*s* resonant Auger spectra. Panel (a) shows the integral intensity of the peak *a* from Fig. 2, the panel (b) peak *b*, and panel (c) displays the intensity of the $KL_{23}L_{23}(^1D)$ final state. The lower panel (d) shows the photoabsorption spectrum (recorded in a total photocurrent mode).

its binding energy is constant [see Fig. 2(b)]. Such satellites, at higher energies than the normal Auger peaks, typically reflect the screening of the Auger final state by the excited spectator electron.[4] Peak *a* is the strongest in curve 3 in Fig. 2(b), decreases in curve 4, and increases again in curve 5. At higher photon energies this peak gradually loses intensity, and is overlapped by the tail of the very strong $KL_{23}L_{23}(^1D)$ peak. The photon-energy dependence of the integrated intensity of peak *a* is presented in the upper panel of Fig. 3(a), and it confirms that its intensity has two maxima peaked at 1073.7 and 1074.7 eV, i.e., at the energy positions of the weak pre-edge features [Fig. 3(d)]. Note that a similar, but very weak, satellite structure can be observed also for $KL_1L_{23}(^1P)$ and (^3P) Auger peaks [in Fig. 2(a)]. From the presence of such spectator structures, the kinetic energy of which is slightly higher than the kinetic energy of the normal Auger transition and whose binding energy is constant, we conclude that in this pre-edge region the photoabsorption ends up in a well-localized core-hole–excited-electron bound state. Below we call this exciton *A*.

With the increase of the photon energy, another satellite [denoted *b* in Fig. 2(a)] appears on the high-energy side of the main Auger peaks. This can be seen in spectra 4–6 in Fig. 2(a) and spectra 7–11 in Fig. 2(b). As in the case of exciton *A*, this additional high-energy structure in the electron spectra has a constant binding energy, and it exists in all Auger groups. The photon energy dependence of the intensity of satellite line *b* [given in Fig. 3(b)] shows that this satellite feature peaks at the photon energy 1076.8 eV, i.e.,

before the photoabsorption has reached its maximum value. This energy is very close to the binding energy value of Na $1s$ photoelectrons: 1076.7 eV. Thus we can state that inside the comparatively broad first photoabsorption maximum (peaked at 1078 eV) there is an energy region where the localized bound state is created. Below we will call this exciton *B*. A substantial difference between the two excited states, excitons *A* and *B*, is that excitons *A* are created at the photon energies, which are about 2 and 3 eV lower than the binding energy of Na $1s$ photoelectron, while exciton *B* is created at energies where the ionization of the $1s$ level becomes possible.

Note that the spectator shift relative to the main Auger peaks in the case of exciton *A* (approximately 4 eV) is larger than that of exciton *B* (approximately by 3 eV), which implies a more delocalized nature of core exciton *B*.

Figure 2(a) shows the appearance of a weak satellite structure, labeled *s*, accompanying the main $KL_{23}L_{23}(^1D)$ Auger band in the photoemission spectra. The energy difference between the main Auger band and the *s* band (about 11 eV) is close to the energy of the valence exciton [10.6 eV (Ref. 12)]. Two different reasons can be responsible for the creation of the observed feature. Peak *s* can be attributed to shake-modified Auger transitions. That is, the Auger decay process of the Na 1s level may be accompanied by a simultaneous excitation of the ligand valence electron to an unoccupied orbital, i.e., by an extra atomic shake-up excitation. This interatomic coexcitation process, however, would be highly improbable in ionic NaF, because the sodium and fluorine atoms are weakly overlapped. In our opinion, it is more probable that peak *s* is due to the inelastic scattering of the Auger electrons inside the crystal. This interpretation is supported by the observation of a satellite structure at 11.1 eV (Ref. 13) in the energy-loss spectra of NaF, which has been ascribed to the creation of a valence-band exciton.

C. Origin of bound states

In atomic sodium the main peak in the $1s$ XAS is ascribed to the transition from $1s$ core level to the unoccupied states of Na $3p$ character.[14] In contrast to atomic sodium, which has a ground-state electronic configuration of $1s^22s^22p^63s$, sodium in highly ionic Na halides has an electronic configuration isoelectronic to the atomic Ne $(1s^22s^22p^6)$. The presence of an additional $(3s)$ electron in the case of an atomic Na causes a variation in the multiplet structure in the $1s$ XAS, in comparison with the structure of the spectra of the Na^+ ion. Therefore, in order to understand the photoabsorption of Na in its halides, the Na $1s$ XAS should be compared with the corresponding spectrum of Ne, which is isoelectronic with Na^+. In the case of a gaseous Ne, $1s\rightarrow 3p$ electric dipole transitions dominate, and the $1s\rightarrow np$ Rydberg series is followed up to $n=6$.[15] The photoabsorption spectrum of a solid neon closely resembles that of a gaseous Ne.[16] By analogy, we infer that $1s\rightarrow np$ transitions play an important role in the Na $1s$ photoabsorption in NaF, and suggest that exciton *B* results from a sequence of transitions $1s\rightarrow 3p$, while a broad maximum at 1078 eV contains contributions from this transition and also from other members of the np series. Then the photoabsorption and the decay process for exciton *B* can be written as the sequence $1s^2\rightarrow 1s^13p\rightarrow 1s^22p^43p$.

The decay of a bound excited state leads to rather pure spectator electronic states. In contrast, the Auger transitions of the exciton *B* state contain significant contributions from the normal Auger spectrum [see Figs. 2 and 3(c)], thus indicating a substantially delocalized or quasibound character of exciton *B*. The evidence of quasibound states in solids was ascribed to an effective potential barrier which hinders the escape of a photoelectron.[17] Then the normal Auger structure in electronic decay spectra of the intermediate excitonic state *B* appears because of the tunneling of the excited electron through the barrier separating the potential well localized around the atom. Thus, the quasibound character of exciton *B* leads to two types of structures in the electron spectra, showing a constant kinetic energy (normal Auger-like behavior) and a constant binding energy (resonant Raman behavior). The ratio of the intensities of the normal and the spectator Auger channels is directly related to the tunneling probability through the potential barrier.

The interpretation of the results presented so far suggests a localized $3p$ origin of the intermediate excitonic state (B). This interpretation is based on the existence of spectator Auger features in decay spectra. An alternative explanation of the creation of the spectator states in the Auger process can be given by considering the recapture of the free photoelectron through the post-collisional interaction (PCI). For atoms this effect was observed in the yield of Ar^+ ions following $2p$ photoionization just above the threshold,[18] and was also explained by a quantum-mechanical theory.[19] This alternative point of view requires no assumption concerning the localization of the intermediate photoexcited state. In light of this interpretation, right above the $1s^2\rightarrow 1s\varepsilon p$ ionization limit, the outgoing photoelectron can be recaptured into a bound state (shake-down) by PCI with a fast Auger electron. Such a decay process would lead to the same final ionic states which should follow the spectator Auger transitions. The intensity of PCI-assisted spectator transitions is sensitive to the width of the initial $1s$ core hole, and should strongly depend on the slope of the absorption edge, on the relative positions of the photoionization threshold, and on the rising edge. Further theoretical work is clearly required to establish whether intermediate excitonic state *B* is quasibound or bandlike.

The situation is also quite complicated in the case of the pre-edge double peak *A* at 1073.7 and 1074.7 eV. When exciton *B* is interpreted as the transition $1s\rightarrow 3p$, it will be natural to consider that band *A* corresponds to the transition $1s\rightarrow 3s$. This is because the Ne-like sodium in the highly ionic NaF has a lower-lying empty $3s$ level. The energy position of the $3s$ level in the Na $1s$ XAS can be estimated as the sum of the energy separation between the Na $2p$ and $1s$ levels, 1040.9 eV (see Table I), and the $2p\rightarrow 3s$ transition energy, 33.13 eV.[20] This estimation leads to an energy value of the $3s$ level of about 1074 eV, which is close to the energy of the first maximum, 1073.7 eV, of band *A*.

The optical transition $1s\rightarrow 3s$ is parity forbidden in a free ion, and is thus not observable in the absorption spectrum of

the atomic neon and sodium. Nevertheless, a weak pre-edge feature similar to the ones observed in NaF was also found in the XAS of a molecular NaF, in clusters of NaF,[21] and in clusters of Ne.[22] The violation of the selection rules was explained by a disruption of symmetry due to an inhomogeneous neighborhood, which introduces a hybridization between the wave functions of $3s$ and $3p$ states, and makes a $1s \rightarrow 3s$ transition possible.[21]

A pre-threshold peak was also observed in the Na $1s$ XAS of NaCl (Ref. 23) at a photon energy of 2 eV below the main photoabsorption maximum. In this case it was suggested that the deformation of the crystal lattice by the assistance of phonons disrupts the symmetry, and therefore makes $1s \rightarrow 3s$ transitions possible. This interpretation was supported by the observation of the temperature dependence of this shoulder. One may consider that thermal vibrations, a possible statistical disorder, defects, and local distortions are also responsible for the transitions $1s \rightarrow 3s$ in NaF. Nevertheless, since the x-ray absorption as well as the electronic decay are fast processes compared to lattice vibrations, the absorbing atom preserves its specific, frozen position during these processes. The symmetry of the absorbing atom after each x-ray-absorption event is different, thus making the p-s hybridization and the $1s \rightarrow 3s$ transition possible.

So far, the splitting of the excitonic structure *A* remains unexplained. The constant binding energy of decay products (peak *a*) shows that both peaks have the same Auger final-ionic states or energetically close spectator Auger final ionic states. It is difficult to ascribe this splitting to a multiplet splitting of the final $1s3s$ configuration, because the magnitude of the observed splitting (about 1 eV) is about four times larger than our calculated value (0.21 eV) in the Hartree-Fock approximation for the energy difference between the $^3S_1$ and $^1S_0$ levels. Nevertheless, it is possible, in principle, to ascribe this double-peak structure wholly or partially to the states of $3d$ origin. In the analysis of the Na $2p$ photoabsorption,[17] it was shown that the hole-electron and crystal-field interaction lower the $3d$-derived states so that they are below the $3p$ level. This allows us to assume that $3d$ states may be at least partially responsible for exciton *A*. Then the double-peak structure in the intensity curve in Fig. 3(a) can be understood as the splitting of the $3d$ states in the crystal field. Further theoretical and experimental work is needed to identify the origin of exciton *A*.

The investigation of the F *KLL* resonant Auger spectra at the F $1s$ photoabsorption edge has shown the existence of two excited states in LiF, NaF, and KF,[6] and has been ascribed to $1s \rightarrow 3p$ and $1s \rightarrow 4p$ transitions. The excitonic contributions at the Na $1s$ photoabsorption edge of NaF cannot be interpreted in this way. First, because of energy considerations, these transitions must be identified as $1s \rightarrow 3s$ and $1s \rightarrow 3p$, respectively. Second, the intensity ratio of the *A* and *B* excitons in NaF, evaluated from the integrated area under the Auger spectator structures (about 1:20), strongly differs from the intensity ratio of $1s \rightarrow 3p$ and $1s \rightarrow 4p$ transitions in the atomic and solid Ne (about 5:1). Moreover, we believe that our present interpretation of the *KLL* resonant Auger spectra at the Na $1s$ photoabsorption edge calls for a reinterpretation of the *KLL* resonant Auger spectra at the F $1s$ edge.

IV. CONCLUSIONS

In this paper, by using synchrotron radiation, we present results of resonant photoemission measurements of NaF across the Na $1s$ photoabsorption threshold. The spectra have been found to exhibit spectator resonant Auger spectator structures at photon energies of 1073.7, 1074.7 and 1076.8 eV. The resonant Auger spectra show that, despite the absence of pronounced structures in the pre-edge region of the Na $1s$ XAS, core-excited localized states are created at these photon energies. Comparisons with the photoabsorption of the atomic Na and Ne have allowed us to conclude that the exciton at 1076.8 eV originates from the $1s^{-1}3p$ states of Na. The possible role of the $1s^{-1}3s$ and $1s^{-1}3d$ states as a cause of excitons at 1073.7 and 1074.7 eV is discussed.

This work was supported by the Estonian Science Foundation, the Crafoord Foundation, and the Royal Swedish Academy of Sciences. The experiments in the MAX-lab were supported by the European Community through the 5th Framework project ''Access to Research Infrastructure Action of the Improving Human Potential Program.'' The authors also wish to thank the staff of the MAX-lab for support.

[1] S. T. Pantelides, Phys. Rev. B **11**, 2391 (1975).
[2] E. L. Shirley, Phys. Rev. Lett. **80**, 794 (1998).
[3] R. Buczko, G. Duscher, S. J. Pennycook, and S. T. Pantelides, Phys. Rev. Lett. **85**, 2168 (2000).
[4] M. Elango, A. Ausmees, A. Kikas, E. Nõmmiste, R. Ruus, A. Saar, J. F. van Acker, J. N. Andersen, R. Nyholm, and I. Martinson, Phys. Rev. B **47**, 11 736 (1993).
[5] H. Wang, J. C. Woicik, T. Åberg, M. H. Chen, A. Herrera-Gomez, T. Kendelewicz, A. Mäntykenttä, K. E. Miyano, S. Southworth, and B. Crasemann, Phys. Rev. A **50**, 1359 (1994).
[6] H. Aksela, E. Kukk, S. Aksela A. Kikas, E. Nõmmiste, A. Ausmees, and M. Elango, Phys. Rev. B **49**, 3116 (1994).
[7] R. T. Poole, J. G. Jenkin, J. Liesegang, and R. C. G. Leckey, Phys. Rev. B **11**, 5179 (1975).
[8] T. Fujikawa, T. Okazawa, K. Yamasaki, J.-C. Tang, T. Murata, T. Matsukawa, and S. Naoe, J. Phys. Soc. Jpn. **58**, 2952 (1989); T. Murata, T. Matsukawa, and S. Naoe, Physica B **158**, 610 (1989).
[9] S. Nakai, M. Ohashi, T. Mitsuishi, H. Maezawa, H. Oizumi, and T. Fujikawa, J. Phys. Soc. Jpn. **55**, 2436 (1986).
[10] E. Hudson, E. Moler, Y. Zheng, S. Kellar, P. Heimann, Z. Hussain, and D. A. Shirley, Phys. Rev. B **49**, 3701 (1994).
[11] E. L. Shirley, J. A. Carlisle, S. R. Blankenship, R. N. Smith, L. J.

Terminello, J. J. Jia, T. A. Calcott, and D. L. Ederer, in *X-Ray and Inner-Shell Processes*, Proceedings of the 18th International Conference, Chicago, Illinois, 1999, edited by R. W. Dunford, D. S. Gemmel, E. P. Kanter, B. Krässig, S. H. Southworth, and L. Young, AIP Conf. Proc. No. 506 (AIP, New York, 2000), p. 283.

[12] K. Teergarden and G. Baldini, Phys. Rev. **155**, 896 (1967).

[13] T. Mabuchi, J. Phys. Soc. Jpn. **57**, 241 (1988).

[14] C. M. Teodorescu, J. M. Esteva, R. C. Karnatak, A. El Afif, and M. Womes, J. Phys. B **30**, 4293 (1997).

[15] M. Coreno, L. Avaldi, R. Camilloni, K. C. Prince, M. de Simone, J. Karvonen, R. Colle, and S. Simonucci, Phys. Rev. A **59**, 2494 (1999).

[16] A. Hiraya, K. Fukui, P.-K. Tseng, T. Murata, and M. Watanabe, J. Phys. Soc. Jpn. **60**, 1824 (1991).

[17] T. Åberg and J. L. Dehmer, J. Phys. C **6**, 1450 (1973).

[18] W. Eberhardt, S. Bernstorff, H. W. Jochims, S. B. Whitfield, and B. Crasemann, Phys. Rev. A **38**, 3808 (1988).

[19] J. Tulkki, T. Åberg, S. B. Whitfield, and B. Crasemann, Phys. Rev. A **41**, 181 (1990).

[20] S. Nakai and T. Sagawa, J. Phys. Soc. Jpn. **26**, 1427 (1969).

[21] C. M. Teodorescu, J. M. Esteva, M. Womes, A. El Afif, R. C. Karnatak, A. M. Flank, and P. Lagarde, J. Electron. Spectrosc. Relat. Phenom. **106**, 233 (2000).

[22] F. Federmann, O. Björneholm, A. Beutler, and T. Möller, Phys. Rev. Lett. **73**, 1549 (1994).

[23] T. Murata, T. Matsukawa, and S. Naoe, Solid State Commun. **66**, 787 (1988).